ACS Photonics

Article

pubs.acs.org/journal/apchd5

Near-Infrared Strong Coupling between Metamaterials and Epsilon-near-Zero Modes in Degenerately Doped Semiconductor Nanolayers

Salvatore Campione,*[,†,‡] Joel R. Wendt,[†] Gordon A. Keeler,[†] and Ting S. Luk*[,†,‡]

[†]Sandia National Laboratories, Albuquerque, New Mexico 87185, United States

[‡]Center for Integrated Nanotechnologies (CINT), Sandia National Laboratories, Albuquerque, New Mexico 87185, United States

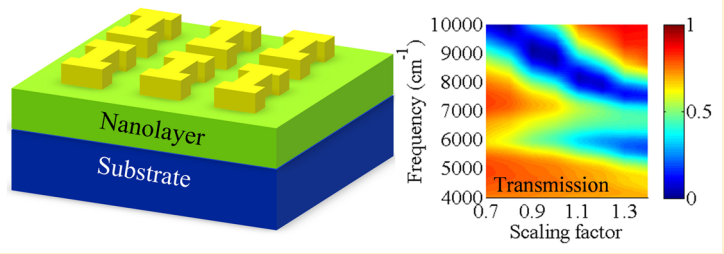

ABSTRACT: Epsilon-near-zero (ENZ) modes provide a new path for tailoring light−matter interactions at the nanoscale. In this paper, we analyze a strongly coupled system at near-infrared frequencies comprising plasmonic metamaterial resonators and ENZ modes supported by degenerately doped semiconductor nanolayers. In strongly coupled systems that combine optical cavities and intersubband transitions, the polariton splitting (i.e., the ratio of Rabi frequency to bare cavity frequency) scales with the square root of the wavelength, thus favoring the long-wavelength regime. In contrast, we observe that the polariton splitting in ENZ/metamaterial resonator systems increases linearly with the thickness of the nanolayer supporting the ENZ modes. In this work, we employ an indium-tin-oxide nanolayer and observe a large experimental polariton splitting of approximately 30% in the near-infrared. This approach opens up many promising applications, including nonlinear optical components and tunable optical filters based on controlling the polariton splitting by adjusting the frequency of the ENZ mode.

KEYWORDS: *strong light−matter interaction, polariton splitting, epsilon-near-zero, nanoresonators, metamaterials, plasmonics, indium-tin-oxide nanolayer, near-infrared*

When two optically resonant systems share the same resonant frequency and are brought together in close proximity, they enter the strong coupling regime when the coupling mechanism dominates competing loss mechanisms. In this regime, the two systems exchange energy periodically at the Rabi frequency. This exchange can be observed in the spectral domain as a splitting of the single cavity resonance into two polariton branches.[1,2] In this situation, these two branches represent two new eigenstates that are a combination of light and matter states. Strong light−matter coupling has been demonstrated experimentally using metallic optical cavities with extremely small interaction volumes.[3−9] Such metallic structures have the ability to confine an electromagnetic field to deep subwavelength volumes. The low quality factors (typically on the order of 10) associated with metallic cavities can be overcome by coupling to systems with large dipole moments. In the infrared wavelength region of the spectrum, metamaterials interacting with intersubband transitions in semiconductor heterostructures[5−10] or with longitudinal phonon modes[11−13] represent preferred choices for strongly coupled systems due to the ease of independently engineering the system parameters. In this work, we investigate a promising strongly coupled system comprising plasmonic metamaterials and epsilon-near-zero (ENZ) polariton modes based on degenerately doped semiconductor nanolayers.

The degree of polariton splitting that can be obtained in a strongly coupled system is a key measure of its suitability for practical applications. In strongly coupled systems based on optical cavities and intersubband transitions, the polariton splitting scales with the square root of the wavelength for a given doping density, effective mass, and number of quantum wells.[1] This wavelength dependence clearly favors the long-wavelength regime. Here, we show that our system, which couples ENZ modes and metamaterial resonators, allows large Rabi splittings even at near-infrared wavelengths.

Natural and artificial ENZ materials have been proposed for exotic optical properties,[14] including optical nanocircuits,[15] optical switching and bistability,[16,17] cloaking devices,[18] highly directional beaming,[19−22] and strong coupling at mid-infrared frequencies.[11−13] It is now clear that deeply subwavelength films support coupled surface modes—ENZ modes—at the frequency where the film's dielectric permittivity vanishes.[23−25] In this work, we strongly couple plasmonic metamaterial resonances and ENZ modes supported by a degenerately doped semiconductor nanolayer (indium-tin-oxide, ITO) at near-infrared frequencies. Both components of the system can be easily engineered: Properties of metamaterial resonators,

Received: November 17, 2015
Published: January 14, 2016

DOI: 10.1021/acsphotonics.5b00663
ACS Photonics 2016, 3, 293−297

including resonance frequency and cavity near-field distribution, depend primarily on the geometry (size and shape) of the individual subwavelength constituents and not on bulk material properties. The ENZ frequency of the ITO nanolayer can be controlled by changing its doping concentration and growth conditions.[26] With this platform, we demonstrate an experimental polariton splitting of approximately 30% at near-infrared frequencies. The only previous experimental realization to date at near-infrared frequencies showed approximately 10% splitting when coupling GaN intersubband transitions to metamaterial resonators.[10] As stated in ref 10, since the intersubband transitions can interact only with the z-polarized component of the electric field, increasing the thickness beyond the penetration depth of the cavity mode cannot further increase the Rabi splitting. However, we observe that the polariton splitting in ENZ/metamaterial resonator systems increases linearly with the thickness of the nanolayer supporting the ENZ modes. Our findings open up many promising applications, including the realization of nonlinear optical components[27] and electrically tunable optical filters.

Consider the structure in Figure 1, where a metamaterial of gold resonators (100 nm thick) is placed on top of an ITO

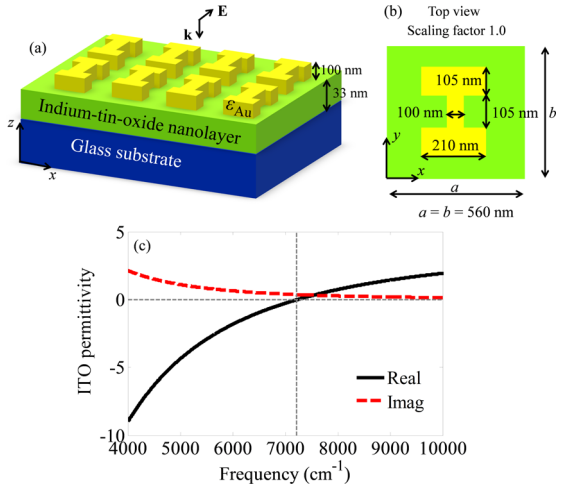

Figure 1. (a) Three-dimensional view of a metamaterial made of dogbone-shaped resonators on top of an indium-tin-oxide nanolayer supporting ENZ modes on top of an alumino-silicate glass substrate for strong coupling purposes (dimensions are not in scale). The normal plane wave illumination, with electric field along y, is explicitly indicated. (b) Top view of the unit cell of the structure in panel (a). Dimensions in nanometers for the spatial scaling factor 1.0 are indicated (when the scaling factor is varied, all the marked unit-cell dimensions in panel (b) are scaled accordingly). (c) Real (solid black) and imaginary (dashed red) parts of the permittivity of the ITO nanolayer versus frequency. The dashed gray lines are a guide to the eye to pinpoint the ENZ crossing of the real part.

nanolayer (33 nm thick) on top of an alumino-silicate glass substrate with relative permittivity $\varepsilon_s = 2.25$. The multilayered sample without gold resonators was purchased from Delta Technologies. The gold permittivity (ε_{Au}) is described using a Drude model:

$$\varepsilon_{Drude} = \varepsilon_\infty - \frac{\omega_p^2}{\omega(\omega + i\gamma)} \quad (1)$$

with parameters extracted from spectroscopic ellipsometry measurements of a 100 nm thin gold film, which yield $\varepsilon_\infty = 1$, a plasma angular frequency of $\omega_p = 2\pi \times 2060 \times 10^{12}$ rad/s, and a damping rate of $\gamma = 2\pi \times 10.9 \times 10^{12}$ rad/s. [The monochromatic time harmonic convention, $\exp(-i\omega t)$, is used here and throughout the paper and is suppressed hereafter.] The ITO permittivity is also described using the model in eq 1 with parameters extracted from spectroscopic ellipsometry measurements, where $\varepsilon_\infty = 4.0824$, $\omega_p = 2\pi \times 440 \times 10^{12}$ rad/s, and $\gamma = 2\pi \times 19.7 \times 10^{12}$ rad/s. The real and imaginary parts of the ITO permittivity are reported in Figure 1c, where it is evident that an ENZ crossing of the real part happens at about 7220 cm^{-1}.

Because of this ENZ crossing, the ITO nanolayer supports an ENZ mode, which is a solution to Maxwell's equations in the

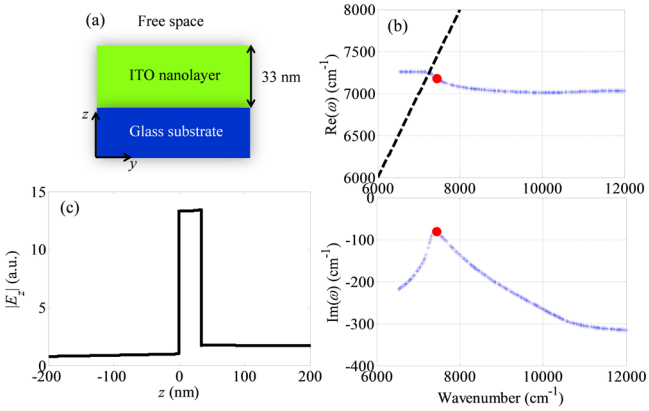

Figure 2. (a) Side view of the 33 nm thick ITO nanolayer on top of a glass substrate supporting an ENZ mode. (b) The dispersion of the ENZ mode computed using eq 2, showing both the real and imaginary parts of ω versus wavenumber. (c) Profile of the magnitude of the z-component of the electric field in arbitrary units versus the spatial variable z computed at $k_\parallel = 7438$ cm^{-1} (e.g., in correspondence with the minimum of $|\mathrm{Im}(\omega)|$), as indicated by the red dots in panel (b).

absence of excitation for the system in Figure 2a. A mode is characterized by a $(k_\parallel,\omega)$ pair that satisfies the equation

$$1 + \frac{\varepsilon_1 k_{z3}}{\varepsilon_3 k_{z1}} = i \tan(k_{z2} d)\left(\frac{\varepsilon_2 k_{z3}}{\varepsilon_3 k_{z2}} + \frac{\varepsilon_1 k_{z2}}{\varepsilon_2 k_{z1}}\right) \quad (2)$$

where $k_\parallel$ is the transverse wavenumber, ω is the angular frequency, ε_i and $k_{zi}^2 = \varepsilon_i \frac{\omega^2}{c^2} - k_\parallel^2$ are the relative permittivity and the longitudinal wavenumber in medium i = free space, ITO, glass with $\mathrm{Re}(k_{zi}) + \mathrm{Im}(k_{zi}) \geq 0$.[28] Equation 2 can be easily derived from either the Fresnel reflection coefficient[29,30] or the transfer matrix method.[31] We select a real-valued $k_\parallel$ and compute the complex-valued ω as suggested in refs 23 and 32. The dispersion of both the real and imaginary parts of ω versus wavenumber $k_\parallel$ computed using eq 2 is shown in Figure 2b for the semiconductor structure depicted in Figure 2a. We observe that the dispersion of the ENZ mode remains quite constant for increasing $k_\parallel$. Moreover, using field-continuity conditions dictated by Maxwell's equations, we compute the magnitude of the z-component of the electric field for $k_\parallel = 7438$ cm^{-1} (e.g., in correspondence with the minimum of $|\mathrm{Im}(\omega)|$), shown in Figure 2c in arbitrary units, which is much stronger than the in-plane components, and remains with a constant profile within the slab.[23] This is the mode to which we want to strongly couple via metamaterial resonators.

DOI: 10.1021/acsphotonics.5b00663
ACS Photonics 2016, 3, 293−297

We then analyze the hypothetical case of resonators on top of the glass substrate with no ITO nanolayer. In such a case, we expect to observe only a metamaterial resonance and no strong coupling properties. We do so, as our aim is to design metamaterial structures whose resonance can be swept across the ENZ frequency of ITO. Figure 3 shows the simulated

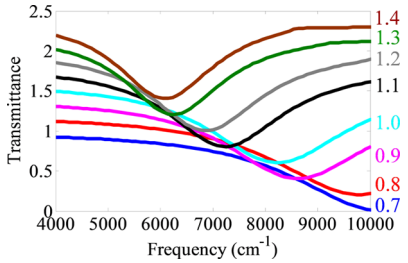

Figure 3. Numerical results for the bare cavity composed of gold metamaterial resonators on top of an alumino-silicate glass substrate with no ITO nanolayer. The figure shows the transmittance spectra for various scaling factors. Each spectrum is vertically shifted by 0.2 for clarity.

transmittance spectra for various scaling factors, obtained from full-wave simulations[33] of the bare cavity on a glass substrate (i.e., with no ITO nanolayer). We simulated a set of metamaterials for which all the spatial unit-cell dimensions in Figure 1b are scaled by a common scaling factor that varied between 0.7 and 1.4 (layer thicknesses are kept unchanged). We observe clearly that the transmittance spectra lack any signature of strong coupling, yet the cavity resonance can be easily swept across 7220 cm^{-1}, the ENZ frequency of the ITO nanolayer.

We then include the ITO nanolayer in the simulations and investigate the properties of the strongly coupled system at near-infrared frequencies. Figure 4 shows the simulated

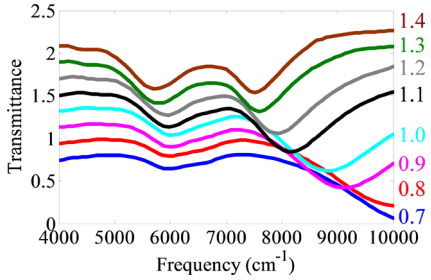

Figure 4. Numerical results for strong coupling between metamaterials and epsilon-near-zero modes at near-infrared frequencies. The figure shows the transmittance spectra for various scaling factors. Each spectrum is vertically shifted by 0.2 for clarity.

transmittance spectra for various scaling factors, obtained from full-wave simulations of the dogbone resonator array on top of the ITO nanolayer on top of a glass substrate. We observe clearly that the transmittance spectra exhibit a polariton splitting around 7220 cm^{-1}, a signature of strong coupling of the metamaterial resonators to the ENZ mode supported by the ITO nanolayer. A splitting of about 2000 cm^{-1} (approximately 30% of the ENZ frequency) is predicted. This is a promising implementation that exhibits a large splitting at near-infrared frequencies, and we proceed next with its experimental verification.

The metamaterial of dogbone resonators is defined by electron beam lithography directly on top of the 33 nm ITO nanolayer. A Ti/Au (5/100 nm) layer is evaporated followed by a standard lift-off process. Similar to the full-wave simulations, we geometrically scale the fabricated metamaterial dimensions to sweep the bare cavity resonance across the ENZ frequency and map out the two polariton branches. A scanning electron micrograph (SEM) image of a fabricated sample is reported in Figure 5a. The transmittance spectra were measured at room

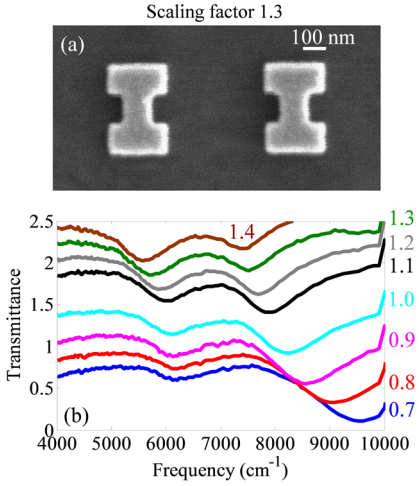

Figure 5. Experimental results for strong coupling between metamaterials and epsilon-near-zero modes at near-infrared frequencies. (a) SEM image of a metamaterial sample (scaling factor 1.3) fabricated with electron-beam lithography. (b) Transmittance spectra for various scaling factors. Each spectrum is vertically shifted by 0.2 for clarity. Good agreement between numerical and experimental results is observed.

temperature using a V-VASE ellipsometer by J. A. Woollam. Figure 5b shows the experimental transmittance spectra for various scaling factors: an experimental splitting of about 2000 cm^{-1} (approximately 30% of the ENZ frequency) is measured. This is a large value of the experimental polariton splitting measured at near-infrared frequencies and represents an important step for future applications. Furthermore, one can note a very good agreement with the simulation results of Figure 4. The minor disagreement between the simulations and measurements can be attributed to fabrication imperfections.

To better highlight the agreement between simulations and experiments, we map the frequencies of upper and lower polaritons versus scaling factor in Figure 6. These frequencies

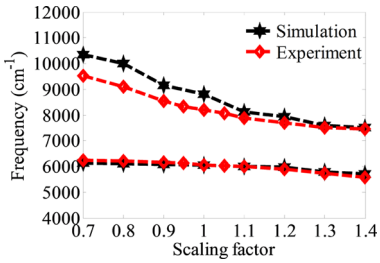

Figure 6. Comparison between simulation and experimental results of the frequencies of upper and lower polaritons of the strongly coupled system. Good agreement between numerical and experimental results is observed.

DOI: 10.1021/acsphotonics.5b00663
ACS Photonics 2016, 3, 293−297

are estimated as the location of the two transmittance minima of the spectra in Figure 4 and Figure 5b. The good agreement between the two results is evident, and this plot further shows the approximately 30% splitting of this strongly coupled system.

We finally show, by plotting the simulated Rabi splitting normalized to the ENZ frequency versus thickness in Figure 7,

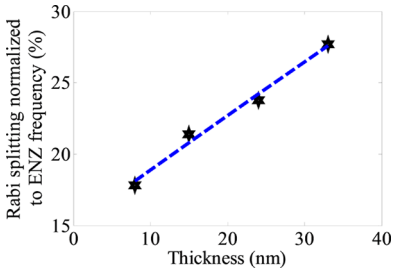

Figure 7. Star symbols represent the Rabi splitting (normalized to the ENZ frequency) dependence on the thickness of the ITO nanolayer. The blue dashed line represents a linear fitting of the data.

that the main parameter that controls the Rabi splitting is the thickness of the ITO nanolayer. We fit the data and observe a linear dependence between Rabi splitting and thickness, as indicated by the blue dashed line in Figure 7. Thus, one can observe that an increase of the thickness leads indeed to an increased Rabi splitting, provided the thickness is in the range of existence of ENZ modes.[25] This result is in agreement with what was recently shown experimentally at mid-infrared frequencies in ref 13. When compared to the structure in ref 10, which achieved a splitting of about 10% for a thickness of 238 nm, we note that our structure achieved a splitting of about 30% with a thickness of only 33 nm. We stress, however, that the linear dependence will cease for larger thicknesses than analyzed here; for example, at a thickness of 50 nm, the Rabi splitting would still be on the order of 30%. This result may indicate that increased absorption begins to dominate the behavior in thicker films, while the large E_z field dictates the response in thinner films, when both thicknesses are in the range where ENZ modes exist. The peak absorption frequency can be tuned slightly as the thickness varies.[30,34]

In conclusion, we have investigated a strongly coupled system at near-infrared frequencies comprising plasmonic metamaterial resonators and ENZ modes supported by ITO nanolayers. Such a platform exhibits a large experimental polariton splitting of approximately 30% at near-infrared frequencies, opening up many possibilities for compelling practical devices and applications. We note that, in place of ITO, one may use other materials including alternative conducting oxides, highly doped semiconductors, nitrides, or 2D conducting materials. In the alternative oxide category, a promising material is cadmium oxide, which has been recently shown to exhibit very low losses.[35]

AUTHOR INFORMATION

Corresponding Authors

*E-mail: sncampi@sandia.gov.
*E-mail: tsluk@sandia.gov.

Notes

The authors declare no competing financial interest.

ACKNOWLEDGMENTS

We acknowledge fruitful discussions with Dr. Michael B. Sinclair and Dr. Igal Brener from Sandia National Laboratories. This work was supported by the U.S. Department of Energy, Office of Basic Energy Sciences, Division of Materials Sciences and Engineering, and performed, in part, at the Center for Integrated Nanotechnologies, an Office of Science User Facility operated for the U.S. Department of Energy (DOE) Office of Science. Portions of this work were supported by the Laboratory Directed Research and Development program at Sandia National Laboratories. Sandia National Laboratories is a multiprogram laboratory managed and operated by Sandia Corporation, a wholly owned subsidiary of Lockheed Martin Corporation, for the U.S. Department of Energy's National Nuclear Security Administration under contract DE-AC04-94AL85000.

REFERENCES

(1) Ciuti, C.; Bastard, G.; Carusotto, I. Quantum vacuum properties of the intersubband cavity polariton field. *Phys. Rev. B: Condens. Matter Mater. Phys.* **2005**, *72*, 115303.
(2) Liberato, S. D.; Ciuti, C. Quantum Vacuum Radiation Spectra from a Semiconductor Microcavity. *Phys. Rev. Lett.* **2007**, *98*, 103602.
(3) Dintinger, J.; Klein, S.; Bustos, F.; Barnes, W. L.; Ebbesen, T. W. Strong coupling between surface plasmon-polaritons and organic molecules in subwavelength hole arrays. *Phys. Rev. B: Condens. Matter Mater. Phys.* **2005**, *71*, 035424.
(4) Todorov, Y.; Andrews, A. M.; Colombelli, R.; Liberato, S. D.; Ciuti, C.; Klang, P.; Strasser, G.; Sirtori, C. Ultrastrong Light-Matter Coupling Regime with Polariton Dots. *Phys. Rev. Lett.* **2010**, *105*, 196402.
(5) Scalari, G.; Maissen, C.; Turcinkova, D.; Hagenmüller, D.; Liberato, S. D.; Ciuti, C.; Reichl, C.; Schuh, D.; Wegscheider, W.; Beck, M.; Faist, J. Ultrastrong Coupling of the Cyclotron Transition of a 2D Electron Gas to a THz Metamaterial. *Science* **2012**, *335*, 1323.
(6) Geiser, M.; Castellano, F.; Scalari, G.; Beck, M.; Nevou, L.; Faist, J. Ultrastrong Coupling Regime and Plasmon Polaritons. *Phys. Rev. Lett.* **2012**, *108*, 106402.
(7) Benz, A.; Campione, S.; Liu, S.; Montano, I.; Klem, J. F.; Allerman, A.; Wendt, J. R.; Sinclair, M. B.; Capolino, F.; Brener, I. Strong coupling in the sub-wavelength limit using metamaterial nanocavities. *Nat. Commun.* **2013**, *4*, 2882.
(8) Dietze, D.; Benz, A.; Strasser, G.; Unterrainer, K.; Darmo, J. Terahertz meta-atoms coupled to a quantum well intersubband transition. *Opt. Express* **2011**, *19*, 13700−13706.
(9) Campione, S.; Benz, A.; Klem, J. F.; Sinclair, M. B.; Brener, I.; Capolino, F. Electrodynamic modeling of strong coupling between a metasurface and intersubband transitions in quantum wells. *Phys. Rev. B: Condens. Matter Mater. Phys.* **2014**, *89*, 165133.
(10) Benz, A.; Campione, S.; Moseley, M. W.; Wierer, J. J.; Allerman, A. A.; Wendt, J. R.; Brener, I. Optical Strong Coupling between near-Infrared Metamaterials and Intersubband Transitions in III-Nitride Heterostructures. *ACS Photonics* **2014**, *1*, 906−911.
(11) Jun, Y. C.; Reno, J.; Ribaudo, T.; Shaner, E.; Greffet, J.-J.; Vassant, S.; Marquier, F.; Sinclair, M.; Brener, I. Epsilon-Near-Zero Strong Coupling in Metamaterial-Semiconductor Hybrid Structures. *Nano Lett.* **2013**, *13*, 5391−5396.
(12) Askenazi, B.; Vasanelli, A.; Delteil, A.; Todorov, Y.; Andreani, L. C.; Beaudoin, G.; Sagnes, I.; Sirtori, C. Ultra-strong light−matter coupling for designer Reststrahlen band New. *New J. Phys.* **2014**, *16*, 043029.
(13) Campione, S.; Liu, S.; Benz, A.; Klem, J. F.; Sinclair, M. B.; Brener, I. Epsilon-Near-Zero Modes for Tailored Light-Matter Interaction. *Phys. Rev. Appl.* **2015**, *4*, 044011.
(14) Engheta, N. Pursuing Near-Zero Response. *Science* **2013**, *340*, 286−287.

DOI: 10.1021/acsphotonics.5b00663
ACS Photonics 2016, 3, 293−297

(15) Engheta, N. Circuits with Light at Nanoscales: Optical Nanocircuits Inspired by Metamaterials. *Science* **2007**, *317*, 1698−1702.
(16) Argyropoulos, C.; Chen, P.-Y.; D'Aguanno, G.; Engheta, N.; Alù, A. Boosting optical nonlinearities in ϵ-near-zero plasmonic channels. *Phys. Rev. B: Condens. Matter Mater. Phys.* **2012**, *85*, 045129.
(17) de Ceglia, D.; Campione, S.; Vincenti, M. A.; Capolino, F.; Scalora, M. Low-damping epsilon-near-zero slabs: Nonlinear and nonlocal optical properties. *Phys. Rev. B: Condens. Matter Mater. Phys.* **2013**, *87*, 155140.
(18) Monti, A.; Bilotti, F.; Toscano, A.; Vegni, L. Possible implementation of epsilon-near-zero metamaterials working at optical frequencies. *Opt. Commun.* **2012**, *285*, 3412−3418.
(19) Gupta, K. C. Narrow-beam antennas using an artificial dielectric medium with permittivity less than unity. *Electron. Lett.* **1971**, *7*, 16−18.
(20) Enoch, S.; Tayeb, G.; Sabouroux, P.; Guérin, N.; Vincent, P. A Metamaterial for Directive Emission. *Phys. Rev. Lett.* **2002**, *89*, 213902.
(21) Lovat, G.; Burghignoli, P.; Capolino, F.; Jackson, D. R.; Wilton, D. R. Analysis of directive radiation from a line source in a metamaterial slab with low permittivity IEEE Trans. *IEEE Trans. Antennas Propag.* **2006**, *54*, 1017−1030.
(22) Alù, A.; Silveirinha, M. G.; Salandrino, A.; Engheta, N. Epsilon-near-zero metamaterials and electromagnetic sources: Tailoring the radiation phase pattern. *Phys. Rev. B: Condens. Matter Mater. Phys.* **2007**, *75*, 155410.
(23) Vassant, S.; Hugonin, J. P.; Marquier, F.; Greffet, J. J. Berreman mode and epsilon near zero mode. *Opt. Express* **2012**, *20*, 23971−7.
(24) Vassant, S.; Archambault, A.; Marquier, F.; Pardo, F.; Gennser, U.; Cavanna, A.; Pelouard, J. L.; Greffet, J. J. Epsilon-Near-Zero Mode for Active Optoelectronic Devices. *Phys. Rev. Lett.* **2012**, *109*, 237401.
(25) Campione, S.; Brener, I.; Marquier, F. Theory of epsilon-near-zero modes in ultrathin films. *Phys. Rev. B: Condens. Matter Mater. Phys.* **2015**, *91*, 121408.
(26) Losego, M. D.; Efremenko, A. Y.; Rhodes, C. L.; Cerruti, M. G.; Franzen, S.; Maria, J.-P. Conductive oxide thin films: Model systems for understanding and controlling surface plasmon resonance. *J. Appl. Phys.* **2009**, *106*, 024903.
(27) Luk, T. S.; de Ceglia, D.; Liu, S.; Keeler, G. A.; Prasankumar, R. P.; Vincenti, M. A.; Scalora, M.; Sinclair, M. B.; Campione, S. Enhanced third harmonic generation from the epsilon-near-zero modes of ultrathin films. *Appl. Phys. Lett.* **2015**, *106*, 151103.
(28) Neviere, M.; Vincent, P. Brewster phenomena in a lossy waveguide used just under the cutoff thickness. *J. Opt.* **1980**, *11*, 153−159.
(29) Born, M.; Wolf, E. *Principles of Optics: Electromagnetic Theory of Propagation, Interference, and Diffraction of Light*; Cambridge University Press, 1999.
(30) Luk, T. S.; Campione, S.; Kim, I.; Feng, S.; Jun, Y. C.; Liu, S.; Wright, J. B.; Brener, I.; Catrysse, P. B.; Fan, S.; Sinclair, M. B. Directional perfect absorption using deep subwavelength low-permittivity films. *Phys. Rev. B: Condens. Matter Mater. Phys.* **2014**, *90*, 085411.
(31) Pozar, D. M. *Microwave Engineering*, 4th ed.; John Wiley and Sons, 2011.
(32) Kliewer, K. L.; Fuchs, R. Optical Modes of Vibration in an Ionic Crystal Slab Including Retardation. II. Radiative Region. *Phys. Rev.* **1966**, *150*, 573−588.
(33) FDTD Solutions by FDTD Lumerical Inc. https://www.lumerical.com/.
(34) Yoon, J.; Zhou, M.; Badsha, M. A.; Kim, T. Y.; Jun, Y. C.; Hwangbo, C. K. Broadband Epsilon-Near-Zero Perfect Absorption in the Near-Infrared. *Sci. Rep.* **2015**, *5*, 12788.
(35) Sachet, E.; Shelton, C. T.; Harris, J. S.; Gaddy, B. E.; Irving, D. L.; Curtarolo, S.; Donovan, B. F.; Hopkins, P. E.; Sharma, P. A.; Sharma, A. L.; Ihlefeld, J.; Franzen, S.; Maria, J.-P. Dysprosium-doped cadmium oxide as a gateway material for mid-infrared plasmonics. *Nat. Mater.* **2015**, *14*, 414−420.

DOI: 10.1021/acsphotonics.5b00663
ACS Photonics 2016, 3, 293−297